Site-selective investigation of site symmetry and site occupation of iron in Fe-doped lithium niobate crystals

Tonya Vitova,[1,a)] Josef Hormes,[1] Matthias Falk,[2] and Karsten Buse[2]

[1]*Institute of Physics, University of Bonn, Nußallee 12, D-53115 Bonn, Germany*
[2]*Institute of Physics, University of Bonn, Wegelerstr. 8, D-53115 Bonn, Germany*

Lithium niobate (LN) crystals, in particular after strong oxidation, are of great relevance for applications in photorefraction and nonlinear optics. Crystals doped with 2 or 4 wt % of iron are studied by extended x-ray absorption fine structure spectroscopy. The Fe atoms are observed to be sixfold coordinated by oxygen atoms and incorporated into the Li site. No evidence for formation of iron oxide clusters is found. *In situ* x-ray absorption spectroscopy measurements of the thermoelectric oxidation of a LN:Fe 2 wt % crystal and the analyses of the partially site-selective x-ray absorption near edge structure spectra of a LN:Fe 4 wt % crystal provide site-selective structural information. We found that the Fe^{2+} and Fe^{3+} sites have the same site symmetries and positions in the LN matrix, i.e., the Fe^{2+} and Fe^{3+} atoms are both octahedrally coordinated by six oxygen atoms and both occupy the Li site. © *2009 American Institute of Physics.*
[DOI: 10.1063/1.3056116]

I. INTRODUCTION

Lithium niobate (LN) ($LiNbO_3$) crystals are an important photorefractive material for applications in nonlinear optics or for holographic data storage.[1,2] In order to increase the refractive index changes, leading to an enhanced storage capacity of holograms, they are doped with transition metals, e.g., Fe, Mn, or Cu. In the case of Fe-doped LN crystals the iron atoms are found in the valence states Fe^{2+} and Fe^{3+}.[3] Upon inhomogeneous illumination, the electrons from the Fe^{2+} impurity centers are excited into the conduction band. They migrate due to drift, diffusion, and bulk photovoltaic effects,[4] and they are finally trapped by Fe^{3+} centers preferentially in the dark areas. The redistributed charge builds up space-charge fields, which modulate the refractive index via the electro-optic effect.

Although light-induced refractive index changes are favorable for some applications, they are undesirable for others and called "optical damage." Some ppm of iron always exist in LN crystals. Upon illumination, refractive patterns develop, which disturb the phase matching conditions and the beam profile in nonlinear-optical applications. One way to avoid the optical damage in a LN crystal is to oxidize it. Recently, a thermoelectric method for very efficient oxidation of Fe^{2+} to Fe^{3+} in LN:Fe crystals has been reported.[5,6]

Precise knowledge about the oxidation state and site occupation of the iron atoms is essential for tuning the photorefractive properties of the LN crystals. A recent x-ray absorption spectroscopy (XAS) study reported the presence of Fe^{2+} and Fe^{3+} atoms in iron-doped LN crystals and their incorporation into the Li site.[7] However, no site-selective structural information was provided, which would allow to differentiate between the Fe^{2+} and Fe^{3+} sites.

The goals of the study presented here are: to determine the incorporation site of the Fe atoms in LN crystals doped with 2 and 4 wt % of Fe (LN:Fe 2 wt %, LN:Fe 4 wt %) by the extended x-ray absorption fine structure (EXAFS) technique, to verify that Fe^{2+} and Fe^{3+} are present in these LN crystals by analyzing x-ray absorption near edge structure (XANES) and visible (VIS) absorption spectra, and to provide site-selective information about the local symmetry and incorporation site of the Fe^{2+} and Fe^{3+} atoms by *in situ* XAS measurements of thermoelectric oxidation of a $LiNbO_3$:Fe 2 wt % crystal, nonresonant high-resolution x-ray emission (HRXE) spectroscopic measurements, and analyses of partially site-selective XANES spectra extracted from a resonant inelastic x-ray scattering (RIXS) map.

II. SAMPLES

The studied samples are iron-doped $LiNbO_3$ crystals supplied by Crystal Technology, Inc. They were grown by the Czochralski technique from a congruent melt that contained 2 or 4 wt % iron oxide (Fe_2O_3). The $LiNbO_3$:Fe 2 wt % and $LiNbO_3$:Fe 4 wt % crystals are notated as C1 and C2 crystals, respectively.

III. EXPERIMENTAL DETAILS

XAS experiments were performed at the INE-Beamline at the ANKA 2.5 GeV synchrotron radiation facility, Karlsruhe, Germany. For details about the instrumentation at this beamline, see Ref. 8. For energy monochromatization, a Lemonnier-type[9] double crystal monochromator equipped with a set of Si(111) crystals was employed. The iron-doped LN crystals were ground, and absorption spectra of the powder samples and the FeO and Fe_2O_3 references were taken at the Fe K edge in fluorescence and transmission modes, respectively. For the measurements in fluorescence mode a five-element Ge solid state detector (Canberra type) was used. During the measurements each sample was positioned

a)Electronic mail: vitova@physik.uni-bonn.de.

on a goniometer; this was rotated 0.001° after each spectrum with respect to the incoming beam, in order to average out the possible diffraction peaks.

All Fe K-edge XANES spectra were measured in the energy interval from 7060 to 7260 eV, with a 0.5 eV step width and 2 s (in fluorescence mode) or 1 s (in transmission mode) integration time. For the EXAFS region equidistant increment was chosen in k space, with 0.03 Å^{-1} step width. At least six XAS (XANES and EXAFS) spectra were collected from the LN:Fe 2 wt % and LN:Fe 4 wt % crystals, in order to check for reproducibility of the spectral features and to improve the counting statistics. For energy calibration, the first inflection point of the K-edge spectrum of an iron foil measured simultaneously was set to the photon energy of 7112 eV. The data reduction in the Fe K-edge XANES spectra consisted of subtraction of a linear background fit to the pre-edge region from 7060 to 7100 eV and normalization of the spectra to an edge jump of one at 7260 eV.

During the *in situ* XAS measurements of the thermoelectric oxidation of a LN:Fe 2 wt % crystal, the monochromator was operated in a quick scanning mode, with 1 min measuring time per EXAFS spectrum. The LN crystal was mounted under 45° with respect to the incoming photon beam. The crystal was put in a furnace in the middle of two perpendicularly crossed quartz tubes. The first tube was directed toward the fluorescence detector. The second tube provided access to the sample for the primary beam. In order to oxidize the crystal thermoelectrically, an electric field was initially applied, where the voltage and the current were restricted to 1000 V and 0.1 mA, respectively. Then the crystal was heated to 700 °C with a ramp of 3.9 °C/min and abruptly cooled down. At room temperature the electric field was switched off.[5]

The measurements of the Fe $K\beta_{1,3}$ and Fe $K\beta'$ emission lines of FeO and Fe_2O_3 references and the RIXS map of the LN:Fe 4 wt % crystal were performed at the wiggler beamline W1 at HASYLAB (Hamburg). For the HRXE measurements, the incident x rays were monochromatized by two Si(111) crystals to the energy of 7500 eV, which is approximately 400 eV above the Fe K edge. X rays scattered from the sample were analyzed by a Johann spectrometer in dispersive geometry,[10] where for the HRXE measurements and the RIXS measurement the sample was moved by 200 and 100 mm, respectively, inside the Rowald circle. A spherically bent Si(531) crystal with radius of curvature of 1 m was employed as an analyzer and a charge coupled device camera (Roper Scientific/Princeton Instruments type) as a position-sensitive detector. The measurements were performed at a Bragg angle $\theta_B = 71.7°$. The experimental energy resolution is estimated as 1.4 eV at the Fe K edge (7112 eV).

The ARTEMIS (Ref. 11) program package was used for EXAFS analyses. The ionization energy (E_0) was chosen as the energy position of the first inflection point of the respective spectrum, i.e., 7124 eV. The XAFS signals $[\chi(k)]$ measured at the Fe K edge, covering a k range from 2.4 to 8.4 Å^{-1}, was Fourier transformed (FT) to R space using a k weighting of 1, 2, and 3 and a Hanning window with window sills dk equal to 2. Fits were performed in R space over a 1.34 Å range. As the initial model the structure of $LiNbO_3$

(Ref. 12) was used. The amplitude reduction factor (S_0^2) was held constant to 0.75, the value obtained for initial fits for a Fe foil FT-EXAFS spectrum measured under the same experimental conditions. While fitting the FT-EXAFS spectra, the S_0^2 parameter was held constant, whereas E_0 ($E_{0(O)}$ and $E_{0(Nb)}$) and the Debye–Waller factors (σ_O^2 and σ_{Nb}^2) were varied. The first coordination shell (Fe–O) was initially fitted by holding the coordination number constant to the model and varying the distance. Then, the coordination number was varied while holding the distance obtained in the initial fit constant. In this way the number of variables was kept 3 for 5.9 independent data points. The number of independent data points are calculated as

$$N_{ind} \sim 2\Delta R \Delta k / \pi, \tag{1}$$

where ΔR and Δk are the range widths of the analysis in R and k spaces, respectively.

In the next step the coordination number and the distance for the first coordination shell were held constant at their values obtained in the first step, and the fit range was extended to 3.4 Å, in order to include the second coordination shell (Fe–Nb). The fit procedure was repeated using two Fe–Nb single scattering paths, but varying one ΔR_{Fe-Nb}. The number of variables was 5 for 8.9 independent data points. For all performed fits, the obtained $\mathfrak{R}$-factor (overall goodness of fit) was 0.01 or better, which means that data and fit agree on average within 1% or better. $\mathfrak{R}$-factor is defined as

$$\mathfrak{R} = \frac{\sum_{i=1}^{N} \{[Re(f_i)]^2 + [Im(f_i)]^2\}}{\sum_{i=1}^{N} \{[Re(\chi_{data_i})]^2 + [Im(\chi_{data_i})]^2\}}, \tag{2}$$

where $N = 2(R_{max} - R_{min})/\delta R + 1$ is the number of points in the data range of the fit and δR is the spacing in R space. f_i is the difference between data and model in R space defined as

$$f_i(R_i) = \chi_{data}(R_i) - \chi_{model}(R_i). \tag{3}$$

The measurement of the absorption coefficient of the 2 wt % iron-doped $LiNbO_3$ crystal was performed at 477 nm in transmission mode using a Cary 500 spectrometer in the VIS spectral range. Using the known relation[3] between Fe^{2+} concentration ($c_{Fe^{2+}}$) and the absorption at 477 nm ($\alpha_{477\ nm}$), $c_{Fe^{2+}} = 2.16 \times 1021\ m^{-2}\ \alpha_{477\ nm}$, the concentration of Fe^{2+} was calculated. An independent measurement by atomic absorption spectroscopy of the $LiNbO_3$:Fe 2 wt % crystal leads to a total iron concentration of 1.11 ± 0.03 wt %.

IV. RESULTS AND DISCUSSIONS

A. EXAFS analyses

The EXAFS spectra in R and k space of the C1 and C2 crystals are plotted along with their best fits in Fig. 1. The structural values obtained by fitting the intense peak at around 1.5 Å (not phase corrected) suggest that the Fe atoms are sixfold coordinated by oxygen atoms in both samples (see Table I). Best fits in the R range up to 3.4 Å were achieved by employing a model with Fe atoms occupying Li sites, i.e., three Nb atoms located at around 3.05 and 3.14 Å for the C1 and C2 crystals, respectively (see Table I). Fits
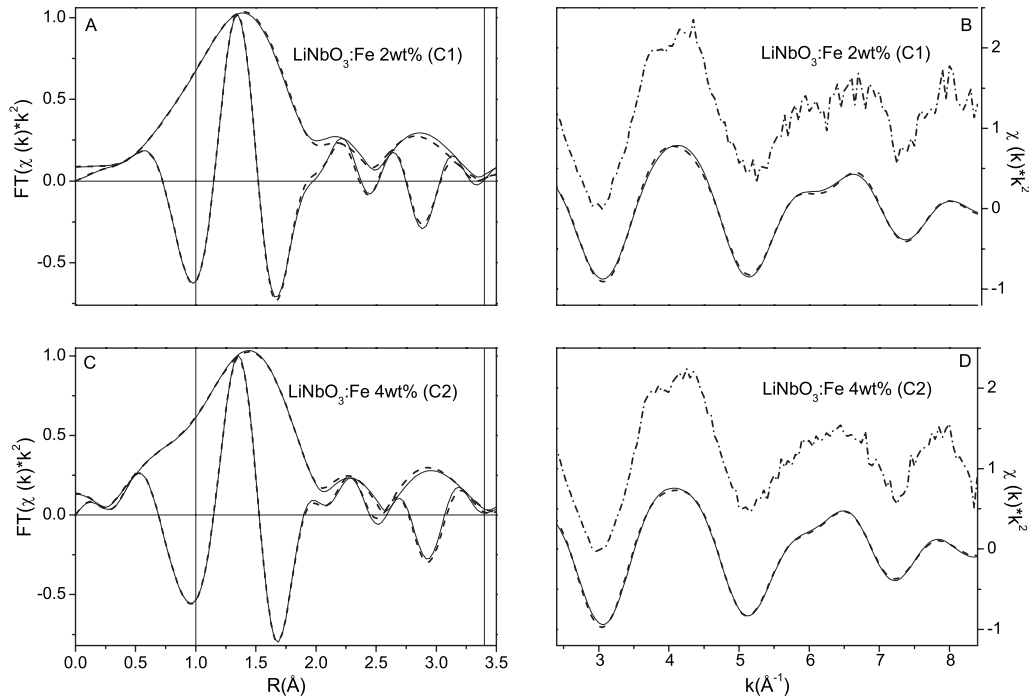
FIG. 1. EXAFS spectra of the [(a) and (b)] LN:Fe 2 wt % and [(c) and (d)] LN:Fe 4 wt % crystals in [(a) and (c)] R (distance) (the magnitude and imaginary part) and [(b) and (d)] k (wave number) [the experimental (dash dot) and Fourier filtered data (solid)] space and their best fits (dash).

using models of Fe_2O_3 clusters and incorporation of Fe atoms into Li and Nb sites yielded unsatisfactory results, which made us confident to rule them out. Results from the EXAFS analysis suggest that the iron atoms are dispersed in the LN:Fe 4 wt % crystal. This contradicts the result of Olimov *et al.*,[7] who reported indications for formation of small iron oxide (Fe_2O_3) clusters in a LN:Fe 4 wt % crystal. The crystal studied in this paper and by Olimov *et al.* originates from the same crystal boule. The discrepancy might be due to the inhomogeneously distributed iron oxide in the boule. This scenario is likely because of the high doping level of iron. The significantly increased Fe–Nb distance in the case of the C2 crystal, from 3.05 to 3.14 Å, provides evidence for distortion of the LN crystal matrix, which might be caused by a decreased distance between the Fe centers.

B. XANES and VIS absorption analyses

Figure 2 depicts the XANES spectra of the C1 and C2 crystals along with those of the FeO and Fe_2O_3 reference compounds. On the energy scale, the spectra of the two samples are positioned close to the spectrum of Fe_2O_3, which indicates a major presence of Fe^{3+} and a minor presence of Fe^{2+} in both crystals. This qualitative estimate is supported by the VIS absorption result, which found 20% of Fe^{2+} and 80% of Fe^{3+} in the 2 wt % iron-doped LN crystal. The energy positions of the absorption edge of Fe in the two samples, determined as the maximum of the first derivative of the respective XANES spectrum, are identical. This finding implies similar Fe^{2+} to Fe^{3+} ratio in the C2 crystal.

The overall shape of a XANES spectrum reflects the electronic and geometrical structure of both Fe^{2+} and Fe^{3+} sites, which makes the extraction of site-selective structural information difficult. The *in situ* thermoelectric oxidization of LN:Fe 2 wt % aimed not only to track the structural changes around the Fe atoms during the oxidation process but also to enable the assignment of spectral features to one of the two sites (Fe^{2+} and Fe^{3+}).

TABLE I. The results from the EXAFS analyses of the LN:Fe 2 wt % (C1) and LN:Fe 4 wt % (C2) spectra and the values of the structural parameters of the used Fe-into-the-Li-site model. The structural parameters are named as follows: N denotes coordination numbers, R (Å) denotes distances, σ^2 (Å^2) denotes Debye–Waller factors, and ΔE_0 (eV) denotes energy shift of the ionization potential.

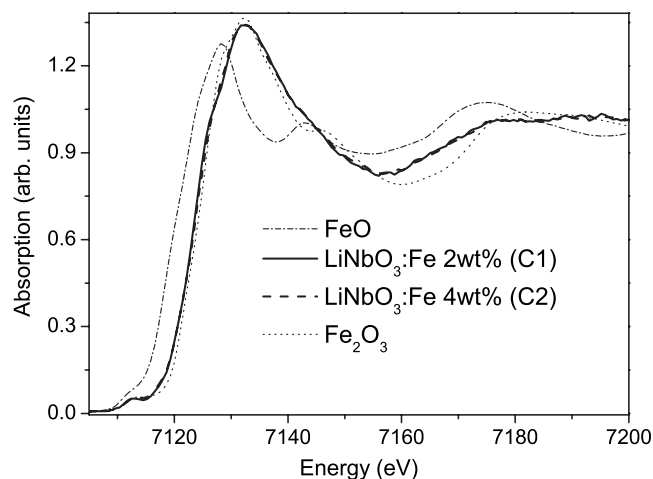|	LN:Fe 2 wt % (C1)				LN:Fe 4 wt % (C2)				Used model: Fe-into-the-Li site	
	R (Å) ±0.01	N	σ^2 (Å^2) ±0.001	ΔE_0 (eV)	R (Å) ±0.01	N	σ^2 (Å^2) ±0.001	ΔE_0 (eV)	R (Å)	N
O^1	1.98	6.6 ± 0.5	0.011	−3.4 ± 0.4	2.00	6.9 ± 0.6	0.012	−2.2 ± 0.3	2.07	3
O^2									2.24	3
Nb^1	3.01	1	0.011	−3.4 ± 0.4	3.10	1	0.012	2.0 ± 0.9	3.01	1
Nb^2	3.05	3.3 ± 0.6	0.011	−3.4 ± 0.4	3.14	2.1 ± 0.6	0.012	2.0 ± 0.9	3.05	3
O^3	3.28	3	0.011	−3.4 ± 0.4					3.29	3

FIG. 2. Fe *K*-edge XANES experimental spectra of the LN:Fe 2 wt % and LN:Fe 4 wt % crystals, and the FeO and Fe$_2$O$_3$ references.

C. *In situ* studies

During thermoelectric oxidization, iron-doped LN crystals change their color from completely black to completely transparent.[5] This fingerprint was the first sign for successful oxidation of iron in the LN:Fe 2 wt % crystal investigated in our *in situ* experiment. In Fig. 3, the XANES spectra, measured at the beginning (S_first) and at the end (S_ last) of the oxidation treatment are shown. A 0.5 eV energy shift of the S_last spectrum toward higher energies, compared to the S_first spectrum, was detected. The 0.5 eV energy shift is measured as the difference in energy positions of the first inflection points of the two spectra, which are defined as the maximum of the first derivative of the respective XANES spectrum. The change in color and the energy shift of the spectrum toward higher energies indicate the successful oxidation of the crystal. However, the XANES spectrum does not show any other changes during the oxidation process, except this energy shift. Moreover, no significant differences were found in the measured EXAFS spectra. These findings suggest that both sites are most likely sixfold coordinated by oxygen atoms, and that the Fe^{2+} and Fe^{3+} atoms occupy the
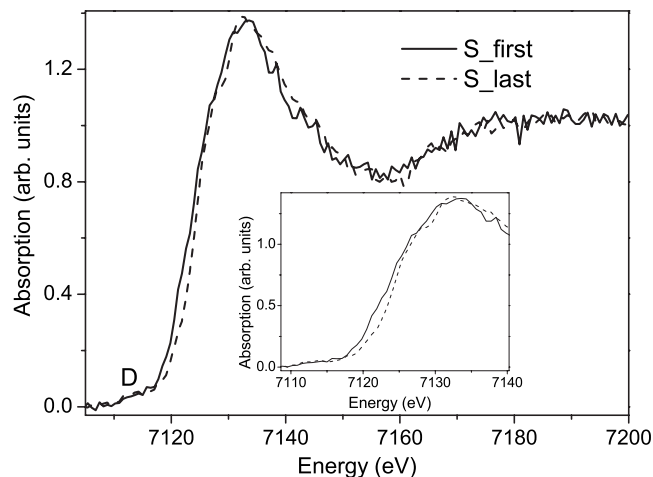

FIG. 3. The first (S_first) and the last (S_last) from the Fe *K*-edge XANES experimental spectra recorded during the *in situ* thermoelectric oxidation of a LN:Fe 2 wt % crystal.
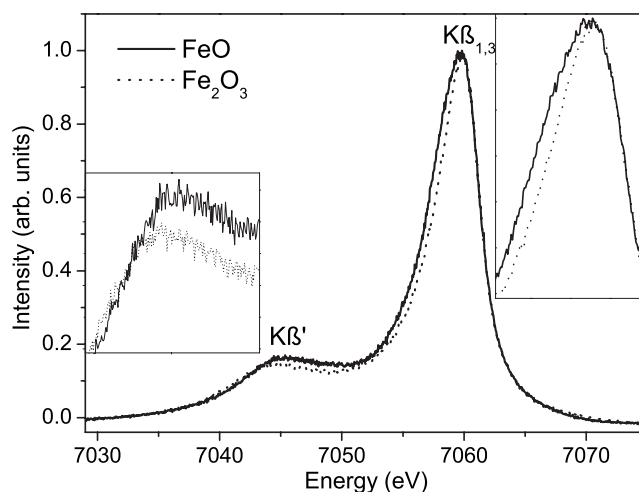

FIG. 4. The HRXE spectra of the FeO and Fe$_2$O$_3$ reference compounds. The insets are enlargements of the *Kβ'* and *Kβ* lines.

Li site. Despite the similarities in short and long range geometrical structures, the electronic structure of the Fe atoms in the two valance states differs. The resonance at the pre-edge region of the S_first and S_last spectra [seen in Fig. 3(d)] is assigned to the transition of the 1*s* electron to the lowest unoccupied states, and it is expected to reflect electronic structural changes. However, the low signal-to-noise ratio and the restricted resolution of a conventional XANES measurement prevent detection of such differences. In order to overcome these limitations, partially site-selective XANES spectra were extracted from a high-resolution RIXS map employing the chemical sensitivity of the high-resolution *Kβ* emission lines of iron oxides with different oxidation states of iron.

D. HRXE spectra and RIXS map

The 1*s*3*p* nonresonant HRXE spectra of FeO and Fe$_2$O$_3$ are displayed in Fig. 4. The *Kβ* line is split into a main intense emission line *K$\beta_{1,3}$*, which reflects 3*p*-1*s* spin down transitions and a satellite *Kβ'* on the low energy site, which reflects 3*p*-1*s* spin-up transitions. The spin selectivity of the *Kβ* emission line has been explained with the exchange interaction between the unpaired spin-up electrons in the 3*d* state and the net 3*p* electron spin after transition of a 3*p* electron to the 1*s* state.[13–16] Since the energy difference between the two emission lines, the width of the *K$\beta_{1,3}$* line, and the intensity of the *Kβ'* line depend on the number of spin-up electrons in the 3*d* state, the 1*s*3*p* HRXE spectra are sensitive to the oxidation state of iron (see Fig. 4). Using the chemical sensitivity of the 1*s*3*p* emission lines, Glatzel *et al.*[17] measured site-selective EXAFS spectra of a mixed-valence compound Prussian blue, which contains Fe^{2+} and Fe^{3+}. By following this approach, we tried to extract site-selective XANES spectra, called A and B, from the RIXS map of the C2 crystal by fixing the emission energy at the low and high energy sides at half-maximum of the *K$\beta_{1,3}$* emission line of the C2 crystal (see Figs. 5 and 6). Since the emission line of the Fe^{2+} reference (FeO) is wider than that of the Fe^{3+} (Fe$_2$O$_3$) reference (Fig. 4), mainly Fe^{2+} is expected to contribute to the A XANES spectrum. As the Fe^{2+}
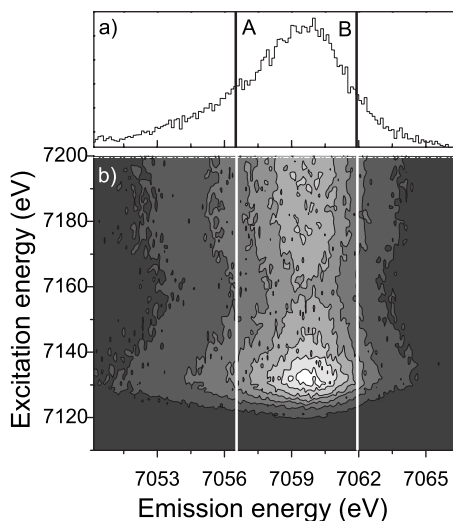
FIG. 5. (a) The $K\beta_{1,3}$ emission line and (b) the $1s3p$ RIXS map of the LN:Fe 4 wt % (C2) crystal.

and Fe^{3+} emission lines overlap, it is not possible to extract "pure" site-selective spectra with the available energy resolution. The A and B XANES spectra are plotted in Fig. 6. Despite the similarity of the two spectra, clear differences in the intensities and center of gravity of the two pre-edges are present (see the inset in Fig. 6). The two pre-edges are isolated by fitting a spline function and subtracting the remaining part of the spectra. The pre-edge resonances of the A and B spectra were modeled with Gauss profiles [see inset (a) in Fig. 6]. The Gauss profiles are not assigned to any atomic transitions. The aim of the fit is the determination of the center of gravity of the two structures. Wilke *et al.*[18] showed in their systematic study of iron oxides that the center of gravity of the pre-edge feature for Fe^{2+} and Fe^{3+} compounds differs by ≈ 1.4 eV. This finding does not depend on the site symmetry of iron. The difference in center of gravity of the pre-edges of the A and B spectra is $\approx 1.4 \pm 0.1$ eV. This result indicates that in the A and B spectra dominantly con-
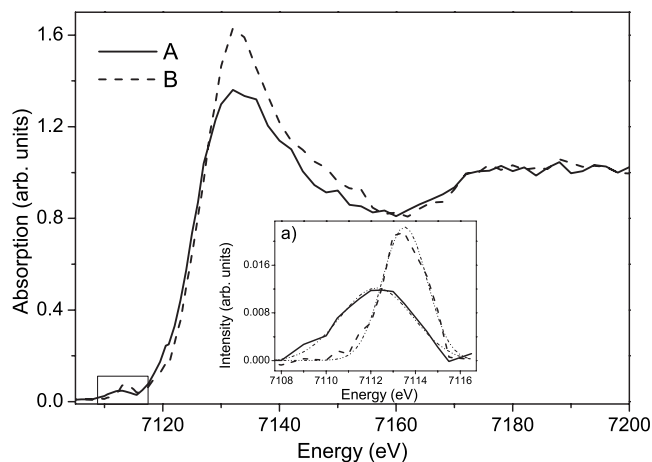

FIG. 6. Site-selective Fe K-edge XANES spectra A and B extracted from the RIXS map of the LN:Fe 4 wt % crystal. The spectra A and B are obtained by integrating ± 1 eV around the emission energies marked with A and B in [Fig. 5(a)], respectively. The background subtracted pre-edge resonances of the A and B spectra, their best fits, and the Gauss profiles (dash dot dot) used as models are shown in the inset (a).

tribute Fe^{2+} and Fe^{3+}, respectively. The similarity of the shape of the white lines and the multiple scattering regions of the two spectra suggest that the short range and long range geometrical structures of the two sites are similar. This finding agrees with the results obtained by the *in situ* experiment. However, in this specific case the partially site-selective XANES spectra are more sensitive, demonstrating the difference in the electronic structure of the Fe^{2+} and Fe^{3+} sites.

V. CONCLUSION

Based on XANES, EXAFS, VIS absorption studies, *in situ* measurements of thermoelectric oxidization of a LN:Fe 2 wt % crystal, and HRXE spectroscopic studies, we come to the following conclusions.

(1) The Fe atoms in the LN crystals doped with 2 and 4 wt % iron are sixfold coordinated by oxygen atoms and occupy Li sites. Formation of iron oxide clusters (Fe–O–Fe coordination) was not found within the sensitivity of the EXAFS analyses.

(2) It was possible to distinguish between the Fe^{2+} and Fe^{3+} sites and it was found that their site symmetries and positions in the LN matrix are very similar, i.e., the Fe^{2+} and Fe^{3+} atoms are in octahedral geometry surrounded by oxygen atoms and they both occupy the Li site.

ACKNOWLEDGMENTS

[1]P. Günter and J.-P. Huignard, *Photorefractive Materials and Their Applications* Springer, New York, 2005), Vol. 1; P. Günter and J.-P. Huignard, *Photorefractive Materials and Their Applications* (Springer, New York, 2006), Vol. 2; P. Günter and J.-P. Huignard, *Photorefractive Materials and Their Applications* (Springer, New York, 2007), Vol. 3.

[2]L. Arizmendi, Phys. Status Solidi A **201**, 253 (2004).

[3]H. Kurz, E. Krätzig, W. Keened, H. Engelmann, U. Gonser, B. Discher, and A. Räuber, Appl. Phys. (Berlin) **12**, 355 (1977).

[4]A. M. Glass, D. V. der Linde, and T. J. Negran, Appl. Phys. Lett. **25**, 233 (1974).

[5]M. Falk and K. Buse, Appl. Phys. B: Lasers Opt. **81**, 853 (2005).

[6]M. Falk, J. Japs, T. Woike, and K. Buse, Appl. Phys. B: Lasers Opt. **87**, 119 (2007).

[7]K. Olimov, M. Falk, K. Buse, T. Woike, J. Hormes, and H. Modrow, J. Phys.: Condens. Matter **8**, 5131 (2006).

[8]M. A. Denecke, J. Rothe, K. Dardenne, H. Blank, and J. Hormes, Phys. Scr., T **115**, 1001 (2005).

[9]M. Lemonnier, O. Coller, C. Depautex, J. M. Esteva, and D. Raoux, Nucl. Instrum. Methods **152**, 109 (1978).

[10]E. Welter, P. Machek, G. Dräger, U. Brüggmann, and M. Fröba, J. Synchrotron Radiat. **12**, 448 (2005).

[11]B. Ravel and M. Newville, J. Synchrotron Radiat. **12**, 537 (2005).

[12]ICSD No. 28294.

[13]G. Peng, F. M. F. deGroot, K. Hämäläinen, J. A. Moore, X. Wang, M. M. Grush, J. B. Hastings, D. P. Siddons, W. H. Armstrong, O. C. Mullins, and S. P. Cramer, J. Am. Chem. Soc. **116**, 2914 (1994).

[14]K. Tsutsumi, J. Phys. Soc. Jpn. **14**, 1696 (1959).

[15] A. Meisel, G. Leonhardt, and R. Szargan, in *X-Ray Spectra and Chemical Binding*, edited by F. P. Schäfer, V. I. Goldanskii, and J. P. Toennies, (Springer-Verlag, Berlin, 1989), Vol. 37.

[16] P. Glatzel and U. Bergmann, Coord. Chem. Rev. **249**, 65 (2005).

[17] P. Glatzel, L. Jacquamet, U. Bergmann, F. M. F. de Groot, and S. P. Cramer, Inorg. Chem. **41**, 3121 (2002).

[18] M. Wilke, F. Farges, P.-E. Petit, G. E. Brown, Jr., and F. Martin, Am. Mineral. **86**, 714 (2001).